Computers and Chemical Engineering 94 (2016) 117–127

Contents lists available at ScienceDirect

Computers and Chemical Engineering

journal homepage: www.elsevier.com/locate/compchemeng

# Computational modeling of megakaryocytic differentiation of umbilical cord blood-derived stem/progenitor cells

Javad Hatami[a,b,*], Frederico Castelo Ferreira[a,*], Cláudia L. da Silva[a], Jorge Tiago[b], Adélia Sequeira[b,*]

[a] Department of Bioengineering and iBB-Institute for Bioengineering and Biosciences, Instituto Superior Técnico, Universidade de Lisboa, Av. Rovisco Pais, No 1, 1049-001 Lisbon, Portugal
[b] Department of Mathematics and CEMAT, Instituto Superior Técnico, Universidade de Lisboa, Av. Rovisco Pais, No 1, 1049-001 Lisbon, Portugal

ARTICLE INFO

*Article history:*
Received 27 June 2016
Received in revised form 27 July 2016
Accepted 29 July 2016
Available online 30 July 2016

*Keywords:*
Hematopoietic stem/progenitor cells
Umbilical cord blood
Computational modeling
Megakaryocyte
Platelet

ABSTRACT

Quantifying the effect of exogenous parameters regulating megakaryopoiesis would enhance the design of robust and efficient protocols to produce platelets. We developed a computational model based on time-dependent ordinary differential equations (ODEs) which decoupled expansion and differentiation kinetics of cells using a subpopulation dynamic model. The model described umbilical cord blood (UCB)-derived cell's behavior in response to the external stimuli during expansion and megakaryocytic differentiation *ex vivo*. We observed that the rate of expansion of Mk progenitors and production of mature Mks were higher when TPO was included in the expansion cytokine cocktail and TPO and IL-3 were added during differentiation stage. Our computational approach suggests that the Mk progenitors were an important intermediate population that their dynamic should be optimized in order to establish an efficient protocol. This model provides important insights into dynamics of cell subpopulations during megakaryopoiesis process and could potentially contribute towards the rational design of cell-based therapy bioprocesses.



## 1. Introduction

Megakaryopoiesis is a process by which mature megakaryocytes (Mks) develop from hematopoietic stem/progenitor cell (HSC/HPC). This complex process occurs *in vivo* in the adult bone marrow (BM) niche and includes HSC/HPC commitment, proliferation and differentiation of megakaryocytic progenitors and final maturation of megakaryocytic cells for production of functional platelets (Reems et al., 2010). Platelets play important roles in blood hemostasis and coagulation, angiogenesis, tumor metastasis and immune defense (Leslie, 2010; Rondina et al., 2013). Platelet transfusion is a vital intervention to treat many hematological diseases and it is routinely used in cancer patients under chemotherapy (Stroncek and Rebulla, 2007). Despite arduous efforts to establish an efficient protocol for *in vitro* production of platelets from different sources, these attempts have not been translated to the clinical application (Thon et al., 2015). One of the reasons, among others, is the inability to quantify the effect of different endogenous and exogenous stimuli on the fate of cells during production of platelets *in vitro*. Computational models have demonstrated to be powerful tools for identification of parameters that could be manipulated to achieve consistent and robust cell-response outputs (Viswanathan et al., 2005; Viswanathan and Zandstra, 2003).

*In vivo*, the fate of HSC/HPC is tightly regulated by the cross-talk between HSC/HPC, stromal cells and niche-secreted factors (Boulais and Frenette, 2015; Morrison and Scadden, 2014). Despite great advances in understanding the blood cell production process, the precise mechanism for the commitment of HSC/HPC towards the lymphoid and myeloid lineages is poorly understood (Lai and Kondo, 2006; Laiosa et al., 2006; Seita and Weissman, 2010). The basic assumption that the HSC/HPC commits to each lineage by an irreversible decision process is still under debate (Ceredig et al., 2009; Laiosa et al., 2006; Naik et al., 2013). The classical view of hematopoiesis is a hierarchical tree system where HSC/HPC differentiates to either myeloid or lymphoid lineage (Bryder et al., 2006; Kawamoto et al., 2010). This process is assumed to be unidirectional and the multipotent cells differentiate to progenitor

* Corresponding authors: Department of Bioengineering and iBB-Institute for Bioengineering and Biosciences, Instituto Superior Técnico, Universidade de Lisboa, Lisbon, Portugal and Department of Mathematics and CEMAT, Instituto Superior Técnico, Universidade de Lisboa, Av. Rovisco Pais, No 1, 1049-001 Lisbon, Portugal.
*E-mail addresses:* javad.hatami@tecnico.ulisboa.pt (J. Hatami), frederico.ferreira@ist.utl.pt (F.C. Ferreira), adelia.sequeira@math.ist.utl.pt (A. Sequeira).

http://dx.doi.org/10.1016/j.compchemeng.2016.07.027
0098-1354/

and mature cells by step-wise lineage restriction in which they gradually lose certain lineage differentiation potential and self-renewal ability as they move along the hierarchical system (Kondo, 2010). Though this view has been recently challenged (Notta et al., 2016), it is supported by the observation that the differentiation and lineage commitment is preceded by lowering the level of lineage specific antigen expression in early progenitor cells (Akashi et al., 2003; Cross and Enver, 1997). The development of computational models to describe the hematopoiesis has been driven, in the last three decades, by the clinical importance of HSC/HPC in bone marrow transplantation and its significance as model for system biology studies (Loeffler and Wichmann, 1980; Manesso et al., 2013; Roeder, 2006). The successful use of mathematical modeling and computer simulations, relevant to the clinical application of the hematopoietic system, revealed the power of those computational tools (Whichard et al., 2010). For example, mathematical modeling and model-driven patient data analysis identified the importance of kinetics of leukemia stem-like cells on the clinical outcome of acute myeloid leukemia for individual patients (Stiehl et al., 2015).

Many of the current lab protocols are designed to commit HSC/HPC toward specific cell lineage using micro-environmental cues. Such cues, including soluble growth factors/cytokines, extracellular matrix components, mechanical forces, cell-cell contact or combination of these factors, should be added to the system in a specific time-dependent manner (Kirouac and Zandstra, 2008; Viswanathan and Zandstra, 2003). Cellular, sub-cellular, population dynamics and hybrid models are examples of computational models that have been developed to predict the fate of cells in the hematopoiesis system as function of such cues (Glauche et al., 2007). Cell population models were used to describe the behavior of stem and progenitor cells *in vitro* and *in vivo* (reviewed elsewhere (Viswanathan and Zandstra, 2003)). Generally, these models link the cellular responses to the exogenous stimuli by fitting the cell population parameters to the experimental results. For example, age structured differential equation-based models have been used to simulate hematopoiesis *in vitro* (Caldwell et al., 2015; Kresnowati et al., 2011; Peng et al., 1996; Roeder, 2006). A particular computational model was developed to describe the effect of exogenously added cytokines on the expansion of human cord blood $CD133^+$ cells in an *in vitro* experimental setting (Gullo et al., 2015). This multiscale model included a set of ordinary differential equations (ODEs) that relates the intracellular events with cellular population behavior. In this study, the authors identified the most important cytokines affecting survival, proliferation and differentiation of $CD133^+CD34^+$ cells using their *in silico* model (Gullo et al., 2015). Another study established a stochastic model of hematopoiesis that predicts the fate of HSCs as a result of cell-cell cross-talk. This stochastic model provided novel insights into the role of intracellular signaling and cell-cell feedback as dominant factors controlling stem cell growth (Kirouac et al., 2009).

To our best knowledge, there is no computational model available in the literature that describes the effects of micro-environmental factors on the cell fate in the megakaryopoiesis process. We previously developed a two-stage protocol for an efficient expansion and differentiation of HSC/HPC, from human umbilical cord blood (UCB) cells, towards the megakaryocytic lineage in a co-culture system with human mesenchymal stem/stromal cells (MSC) (Hatami et al., 2015, 2014). The aim of the present work was to develop a computational framework to quantitatively represent such a complex and dynamic system of megakaryopoiesis *ex vivo*. We developed a system of ODEs that describes the temporal kinetic of the expansion and the differentiation of HSC/HPC. The unknown kinetic constants (cell fate rate coefficients) were obtained by fitting the analytical solution obtained from ODEs to the average response of cell subpopulations from the *ex vivo* culture of HSC/HPC. This approach aims to provide a systematic understanding of the synergic effect of different biological and chemical agents present in the BM niche on the outcome of megakaryopoiesis process.

## 2. Materials & methods

### 2.1. Cell isolation, expansion and differentiation

UCB isolation, expansion and differentiation were performed according to our previous work (Hatami et al., 2015), which provided a superior protocol for the megakaryocytic differentiation of HSC/HPC *ex vivo*. Briefly, UCB samples were obtained from healthy donors and low-density mononuclear cells (MNC) were separated by means of a Ficoll density gradient. Mitomycin C-treated bone marrow (BM)-derived-MSCs (BM-MSCs) were used as a feeder layer (*Feeder*) in co-culture (direct cell-cell contact) during the expansion stage and on selected conditions during differentiation stage.

UCB $CD34^+$-enriched cells were expanded at the initial density of $3.0 \times 10^4$ cells/mL. QBSF-60 (Quality Biological Inc) was used as a culture medium for both expansion and differentiation stages. A pool of UCB MNC (*i.e.* from different donors), enriched for CD34 expression by magnetic activated cell sorting (MACS), was used in co-culture with BM-MSC (direct cell-cell contact) for the expansion stage. Two cytokine cocktails named Z9 and T0, optimized in our previous works (Andrade et al., 2010; Hatami et al., 2015), were supplemented to the culture medium in the expansion stage. Z9 contains SCF (60 ng/mL), Flt-3 (55 ng/mL), TPO (50 ng/mL) and basic fibroblast growth factor (b-FGF) (5 ng/mL) and T0 contains SCF (60 ng/mL), Flt-3 (75 ng/mL) and b-FGF (5 ng/mL) (all from Peprotech, supplied by Tebu-bio, Alges, Portugal).

For differentiation stage, cells were firstly expanded for 7 days using Z9 cocktail and in co-culture with BM-MSC. Then, the expanded cells were cultured for additional 10 days at the initial density of $2.0 \times 10^5$ cells/mL. Three conditions were assessed in the differentiation stage: (i) using a mitomycin-treated BM-MSC feeder without any cytokine addition (*Feeder*); (ii) in culture medium supplemented with IL-3 and TPO (both from Peprotech) at concentrations of 10 ng/mL and 100 ng/mL, respectively, without a feeder layer co-culture (*Cyt*); and (iii) using both mitomycin-treated BM-MSC as the feeder layer with addition of cytokine IL-3 and TPO at the previously mentioned concentrations (*Cyt + Feeder*). All the expansion and differentiation experiments were performed at least in triplicate.

### 2.2. Proliferative and phenotypic analysis

The Trypan blue (Gibco) dye exclusion method was used to estimate cell numbers and viability. Flow cytometry (FACSCalibur equipment, BD) was used for phenotypic analysis as previously described (Hatami et al., 2015, 2014). Briefly, cells were labelled with a panel of monoclonal antibodies including anti-CD34 (for early HSC/HPC), CD41 (for megakaryocytic lineage) and CD42b (for mature megakaryocytic cells). Total number of cells was multiplied by the percentage of that specific subpopulation, obtained from flow cytometry data, to estimate each subpopulation cell numbers. Results are presented as a mean ± standard error of mean (SEM).

## 3. Computational framework

In order to understand the evolution of different subpopulations during the expansion and differentiation stages, we developed a computational framework to decompose population-averaged time-course information into subpopulation-specific rate parameters. Our model conceptualized the lineage commitment of HSC/HPC to megakaryocytic and non-megakaryocytic lineage

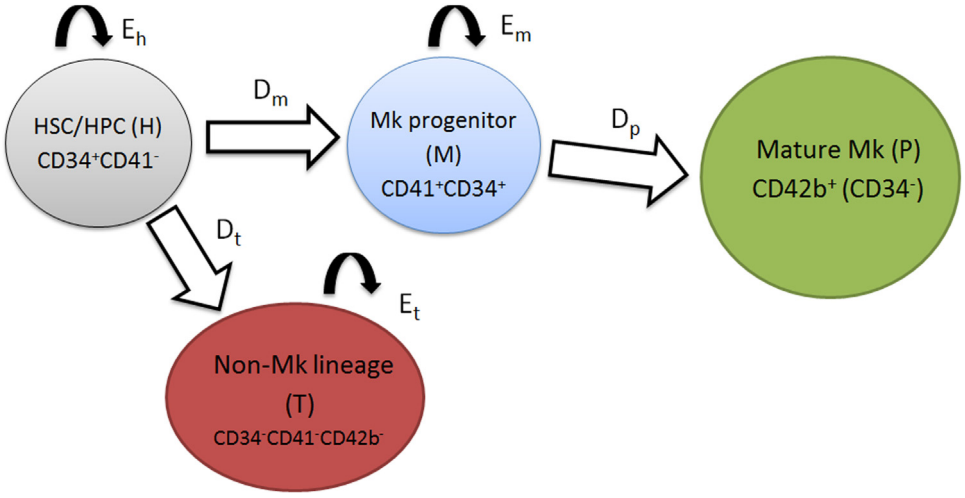


**Fig. 1.** Schematic representation of four cell states during HSC/HPC commitment to Mk and non-Mk lineages. Cell surface markers were used to distinguish between different cell states. Number of non-Mk lineage cells (T) were calculated based on subtraction of the total number of cells in megakaryopoiesis pathway from the total number of cells (TCN) at each time point (*e.g.* T = TCN-H-M-P). Expansion (E) and differentiation (D) rates are presented by black and white arrows, respectively.

as schematically illustrated by Fig. 1. The multipotent HSC/HPC differentiates into the progenitor and mature cells which this process is assumed to be unidirectional. Four main elements were defined for the description of the system; HSC/HPC (H), megakaryocytic progenitors (M), mature megakaryocytic cells (P) and non-megakaryocytic cells (T), which were determined by the phenotypes $CD34^+CD41^-$, $CD34^+CD41^+$, $CD42b^+CD34^-$ and $CD34^-CD41^-CD42b^-$, respectively (Deutsch and Tomer, 2013; Pineault and Boisjoli, 2015; Psaila et al., 2016). The topology of our model was in agreement with other studies which demonstrated in infants Mk cells are directly branched from multipotent stem cell and not from oligopotent progenitors-like CMP (common myeloid progenitors)(Notta et al., 2016).

In this model, "E" and "D" are expansion and differentiation rates, respectively (Fig. 1). The constant "E" is the net rate of proliferation and death of each subpopulation. The description of all cell fate rate coefficients is presented in Table 1. The following assumptions were considered in the computational model: (i) Coefficient rates of proliferation and differentiation during the experimental time frame were constant; (ii) HSC/HPCs were a multipotent stem/progenitor cell population and therefore had (limited) self-renewal and differentiation potential; (iii) Non-Mk cells included a heterogeneous population of progenitors/precursors and mature cells in lymphoid, as well as other cells in myeloid lineage that did not express specific cell surface markers of Mk lineage (*e.g.* $CD41^-$) nor had the potential to express the CD34 (*e.g.* $CD34^-$), a marker for stem and progenitor cells in the hematopoiesis system; (iv) there was no *trans*-lineage differentiation between Mk and other lineage; and (v) mature megakaryocytic cells (P) were not able to neither proliferate nor differentiate.

We applied cell balance equations to our system considering the number of cells in each state (Bartolini et al., 2015; da Silva et al., 2003) to derive four ODEs (Fig. 2) and compute the number of each subpopulations over time (da Silva et al., 2003). In the ODEs, the time (t) dependent number of cells are H(t), M(t), T(t) and P(t), representing the number of HSC/HPCs, megakaryocytic progenitors/precursors, non-Mk cells and mature Mk cells, respectively. In this system, there are six coefficients rate (cell fate rate coefficients) including three expansions ($E_h$, $E_t$, $E_m$) and three differentiation ($D_m$, $D_t$, $D_p$) coefficient rates. These coefficients included as the components of a cell fate vector, called "h". Initial conditions are represented by $H_0$, $M_0$, $T_0$ and $P_0$, which define the number of H(t), M(t), T(t) and P(t) at the time zero, respectively (Fig. 2). Time zero corresponds to the begginig of the experiment for the expansion stage. For the differentiation stage, time zero corresponds to the date 7 of the expansion, when the expanded cells were transferred to differentiation stage. In order to fully describe the evolution of subpopulations (C(t) = (H(t),M(t),T(t),P(t))), the values of "h" were estimated for each one of the *ex vivo* cultures using the correspondent experimental data and boundary conditions. Fig. 2 represents a flowchart to obtain the vector 'h' values. Four explicit time-dependent equations to calculate subpopulations cell numbers were obtained by the analytical solution of the established ODEs (see Supplementary material for details):

$$H(t) = H_0.e^{X.t},\ assuming: X = E_h - D_t - D_m \quad (1)$$

$$M(t) = \frac{D_m.H_0}{X-Y}\left(e^{X.t} - e^{Y.t}\right) + M_0.e^{Y.t},\ assuming: Y = E_m - D_p \quad (2)$$

$$T(t) = \frac{D_t.H_0}{X-E_t}\left(e^{X.t} - e^{E_t.t}\right) + T_0.e^{E_t.t} \quad (3)$$

$$P(t) = \frac{D_m.D_p.H_0}{X.Y}\left[\frac{Y.e^{X.t} - X.e^{Y.t}}{X-Y} + 1\right] + D_p.M_0\left[\frac{e^{Y.t}-1}{Y}\right] + P_0 \quad (4)$$

Vector "h" was estimated by minimization of the Least Square error function. This function (err (h)) was obtained by calculating the difference between subpopulation expressions (Eqs. (1)–(4)) and experimental average values for each one of the four subpopulation cell numbers ($C_i$) at 5 different time instants ($t_j$) according to Eq. (5).

$$err(h) = \sum_{i=1}^{4}\sum_{j=1}^{5}\left(C_i\left(t_j, h\right) - C_i^{exp}\left(t_j\right)\right)^2 \quad (5)$$

In Eq. (5), $C_i^{exp}\left(t_j\right)$ represents the experimental data for the subpopulation $i$, at time $t_j$, with $j$ corresponding to the expansion or the differentiation cultivation days. Expansion rate coefficients can have positive or negative values, as they are the net of proliferation and death rates of cells. However, differentiation rate coefficients, by its definition, are always equal or higher than zero. With the different boundary limits, the resultant expansion and differentiation coefficient rates were always in the interval [−1,1] and [0,1], respectively. Therefore, to minimize the computation cost, we selected the intervals [−5,+5] and [0,+5] as boundary conditions for the expansion and the differentiation coefficient rates, respectively.

Two issues must be addressed in order to obtain the vector "h". The first refers to the non-linear dependence of Eqs. (1)–(4)

**Table 1**
Description of cell fate rate coefficients.

| Rate Constant | Description |
|---|---|
| $E_h$ | Expansion coefficient rate of HSC/HPC (H) |
| $E_m$ | Expansion coefficient rate of Mk progenitors (M) |
| $E_t$ | Expansion coefficient rate of non-megakaryocytic cells (T) |
| $D_m$ | Differentiation coefficient rate of HSC/HPC (H) to Mk progenitors (M) |
| $D_t$ | Differentiation coefficient rate of HSC/HPC (H) to non-megakaryocytic cells (T) |
| $D_p$ | Differentiation coefficient rate of Mk progenitors (M) to mature Mk cells (P) |

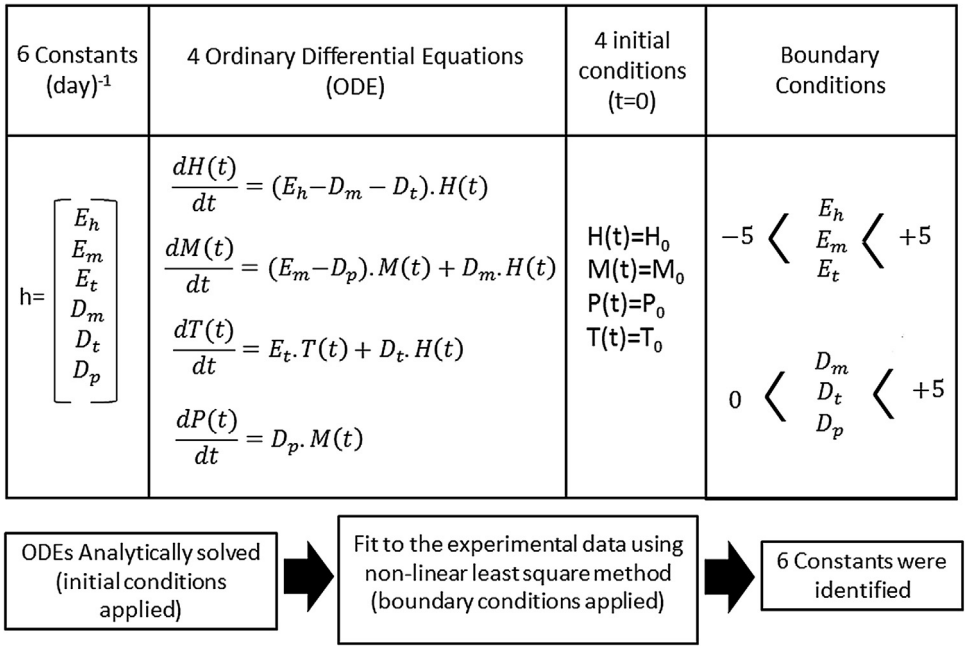


**Fig. 2.** Flowchart presenting four ordinary differentiation equations (ODEs), 6 constants (cell fate rates), initial and boundary conditions that describe the evolution of subpopulation states.

on the unknown vector of coefficient rates "h", and the associated boundary conditions. To tackle this issue, we used the sequential quadratic programming (SQP) solver provided by the MATLAB function "fmincon" as a nonlinear optimization algorithm to find all local minimums. The second issue refers to the fact that we have to find a global minimum for Eq. (5). This issue was handled by using the "Multistart" algorithm from MATLAB, associated to SQP solver. This optimization algorithm generated multiple starting points (500 points in this case), within the established boundary conditions. In this way, the algorithm was able to find the global minimum solution for the problem.

## 4. Results

### 4.1. Effect of TPO addition on cell subpopulation dynamics during the expansion stage

The result of this section is based on our experimental work previously reported (Hatami et al., 2015). UCB-derived $CD34^+$ cells were expanded in co-culture with BM-MSCs using T0 or Z9 cocktail for 14 days. The concentrations of different cytokines in the cocktails Z9 (*i.e.* TPO-containing cocktail) and T0 (*i.e.* TPO-free cocktail) are depicted in Fig. 3-D. Experimental and estimated results were illustrated to visualize the evolution of different subpopulations during the expansion stage (Fig. 3). The higher number of cells expanded using Z9 cocktail emphasizes the enhancing effect of TPO addition to the expansion cocktail on the total number of cells and all subpopulations (Fig. 3).

Normalized error (Nerr) for each subpopulation, calculated according to Eq. (6), were in the range of 7–21% and 11–25% for the cells expanded using the Z9 and T0 cytokine cocktail, respectively.

$$Nerr_i = \frac{\sqrt{(err\,(h))}}{\sqrt{\sum_{i=1}^{4}\sum_{j=1}^{5}\left(C_i^{exp}\,(t_j)\right)^2}} \times 100 \quad (6)$$

### 4.2. Impact of the co-culture with BM-MSC and the addition of cytokines on cell fate rates during differentiation stage

UCB $CD34^+$-enriched cells expanded for 7 days, in co-culture with BM-MSC using Z9 cytokine cocktail, were seeded to the differentiation stage for additional 10 days. The result of the current study demonstrated that the combination of co-culture with BM-MSC (*Feeder*) and addition of *Cyt* (TPO + IL-3) provided a synergic effect to boost the total number of megakaryocytic progenitors (M) and mature Mk cells (P) in comparison to the conditions using only *Feeder* co-culture or *Cyt* addition (Fig. 4). Addition of TPO + IL-3 (*Cyt*) to the differentiation medium in the absence of a MSC feeder layer resulted in a higher number of Mk progenitors (M) and mature Mk cells (P) and a lower number of non-Mk cells (T) in comparison to the condition where expanded cells were differentiated in co-culture with BM-MSC (*Feeder*) in the absence of TPO + IL-3, which indicates the superiority of these cytokine-driven signaling for the megakaryocytic differentiation.

Experimental and estimated results were outlined to visualize the effect of *Cyt* addition and co-culture with the feeder layer during the differentiation stage on the different subpopulations cell

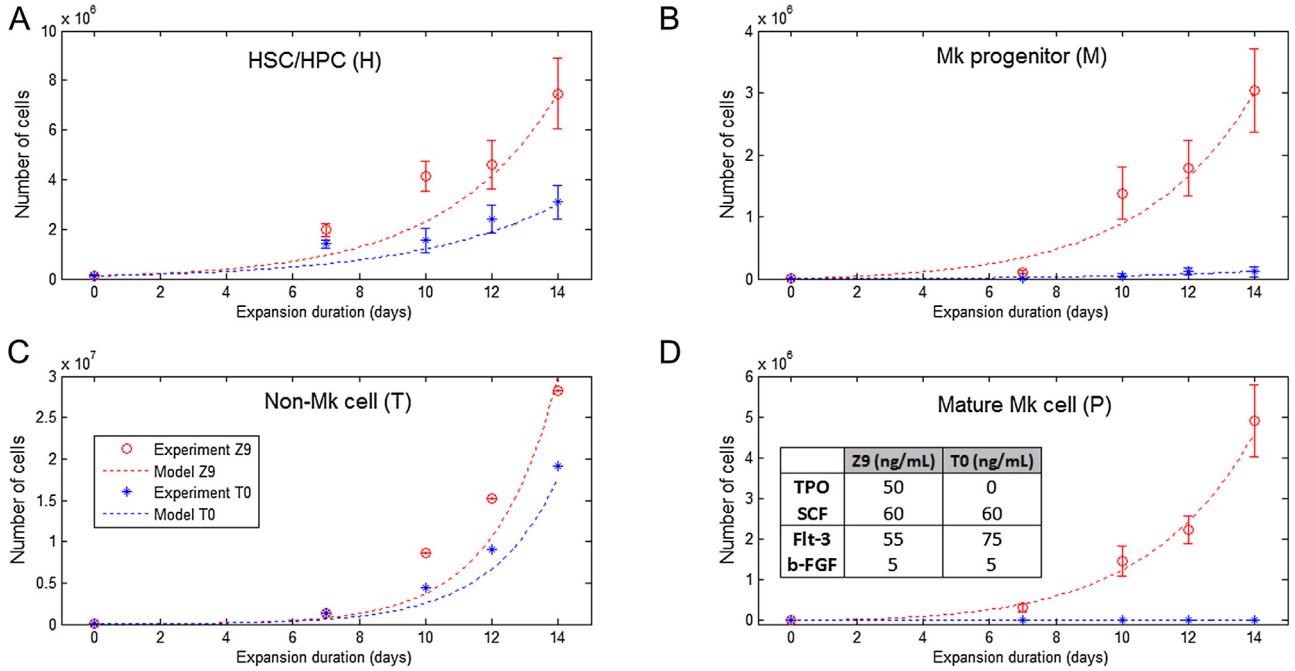


**Fig. 3.** A) Total number of HSC/HPC (H), B) Mk progenitors (M), C) non-Mk lineage cells (T) and D) mature Mk cells (P) are presented as function of time (days) during 14 days of the expansion stage. This outcome was the result of expansion in co-culture with BM-MSC using the two cytokine cocktail Z9 and T0. D) The cytokine composition of Z9 and T0 cocktails are presented in a table. The experimental data (Experiment) obtained using Z9 and T0, outlined as average ± SEM ($n \geq 3$), are represented by red circles and blue crosses, respectively. Estimated curves (Model) fitted to the experimental data for Z9 and T0 conditions are sketched in red and blue dotted lines, respectively. (For interpretation of the references to colour in this figure legend, the reader is referred to the web version of this article.)

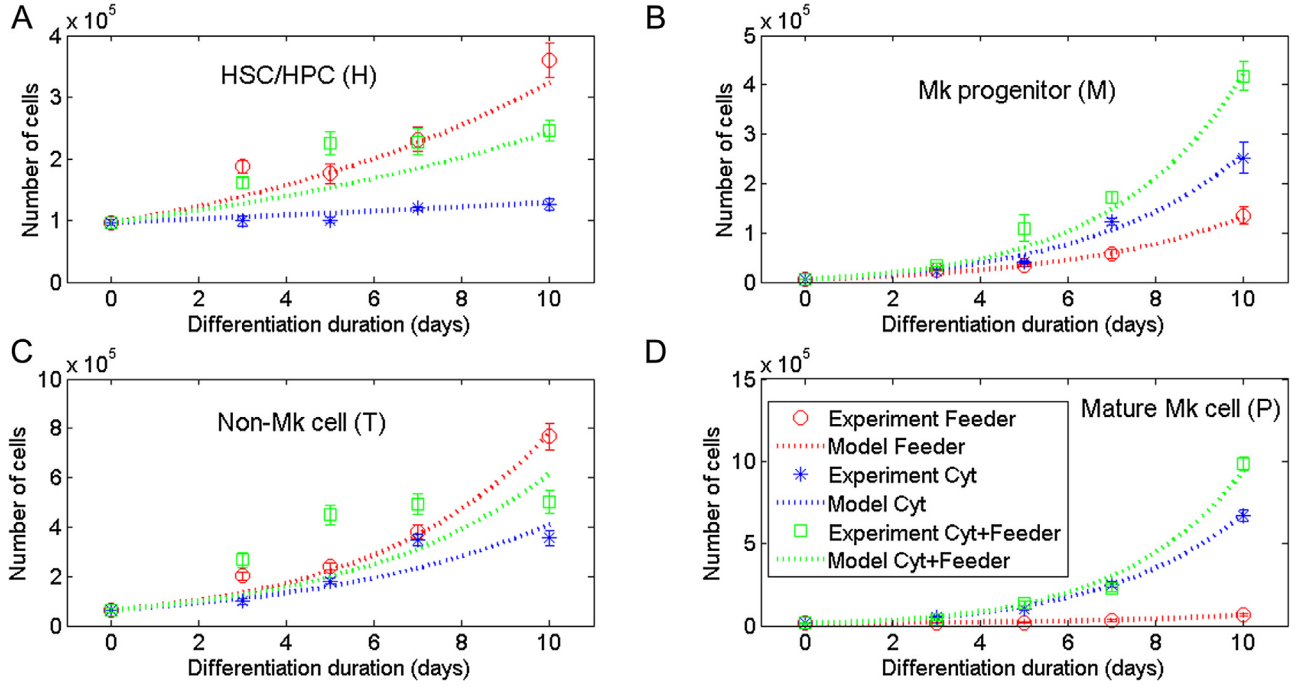


**Fig. 4.** A) Total number of HSC/HPCs (H), B) Mk progenitors (M), C) non-Mk lineage cells (T), and D) mature Mk cells (P) are presented as a function of time (days) during 10 days of the differentiation stage. This outcome was the result of 7 days expansion in co-culture with BM-MSC using the Z9 cocktail and then 10 days of differentiation using cytokine addition (Cyt-blue color) or in co-culture with BM-MSC (Feeder-red color) or combination of the two conditions (Cyt + Feeder- green color). The experimental data (Experiment), presented as average ± SEM ($n \geq 3$), and estimated curves (Model), fitted to the experimental data, are outlined as circles and dotted lines, respectively. (For interpretation of the references to colour in this figure legend, the reader is referred to the web version of this article.)

numbers (Fig. 4). The normalized errors, calculated according with Eq. (6) for the cells expanded for 7 days using the Z9 cocktail and then differentiated in co-culture with a BM-MSC feeder layer with addition of cytokines (*Feeder + Cyt*), or differentiated only in the presence of BM-MSC feeder layer (*Feeder*) or differentiated only by addition of cytokines (*Cyt*), were in the range of 7–37%, 5–9% and 2–20%, respectively. The computational model developed herein underpredicted the number of cells in the *Feeder + Cyt* condition for non-Mk and HSC/HPC populations (Fig. 4A & C-green dotted lines). Moreover, for this particular set of data, the shape of the curve pre-

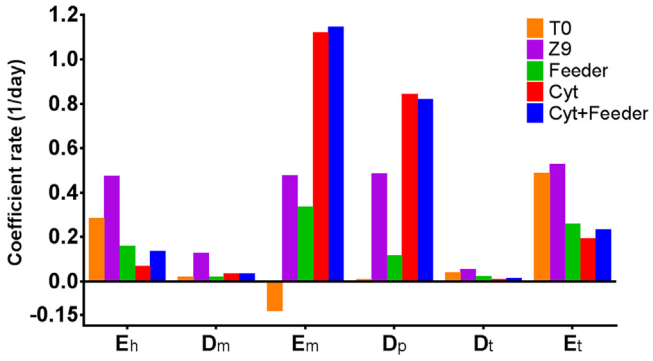


**Fig. 5.** Cell Fate rates as the result of the expansion (labelled as T0 and Z9) and the differentiation stage (labelled as Cyt, Feeder and Cyt + Feeder). Expansion stage was performed for 14 days using Z9 and T0 conditions in co-culture with BM-MSC feeder layer. Cells expanded in Z9 for 7 days were differentiated for additional 10 days using cytokines addition (Cyt) or in co-culture with BM-MSC (Feeder) or the combination of the two conditions (Cyt + Feeder).

dicted by the model was different compare to the experimental data.

Cell fate rate coefficients were calculated and are presented in Fig. 5 to study (i) TPO inclusion in the cytokine cocktail supplemented in the expansion stage (using T0 *vs* Z9 cocktails), (ii) addition of TPO and IL3 (*Cyt*) and (iii) co-culture with BM-MSC (*Feeder*), as well as combination of *Cyt + Feeder* in the differentiation stage. The presence of the TPO in the Z9 cocktail, during expansion stage, enhanced all 6 coefficient rates of the expansion and differentiation in comparison to the T0 cocktail (Fig. 5). The rate of production of mature Mk cells ($D_p$) was significantly higher when TPO was included in the expansion cocktail compared to the cells expanded using TPO-free condition (*e.g.* $D_p$,Z9/$D_p$,T0 = 160 1/day).

The non-specific signaling of BM-MSC, as a feeder layer, for Mk lineage commitment in comparison to TPO + IL-3 (*Cyt*), resulted into the lowest percentage and number of $CD41^+$ cells observed in the differentiation stage with lower expansion rates of Mk progenitors, lower rates of differentiation of HSC/HPC to Mk lineage and smaller rates of differentiation of Mk progenitors into mature Mk cells (*e.g.* $E_m$, $D_m$, $D_p$: Cyt > Feeder). This result supports our previous empirical findings, that is, the supremacy of *Cyt* addition over *Feeder* signaling to have an efficient Mk differentiation process (Hatami et al., 2015). The synergic effect of *Cyt + Feeder* resulted in higher rates of expansion of Mk progenitors ($E_m$) and higher rates of differentiation ($D_m$ and $D_p$) compared to the condition where only *Feeder* was added to the differentiation protocol.

The TPO-free cytokine cocktail used during the expansion stage, T0, did not have any effect on the early steps of megakaryopoiesis process; for example, when comparing the rates of HSC/HPC differentiation to the Mk progenitors between T0 and *Feeder* condition, no meaningful differences were found ($D_{m,\,T0} = D_{m,\,Feeder}$).

The conditions that cytokines (including TPO) were supplemented during the full time length of the culture (*Cyt + Feed*, *Cyt* and Z9) resulted in higher rates of differentiation ($D_m$ and $D_p$) and expansion ($E_m$) associated with the Mk lineage. This result shows that in order to have a higher commitment rate toward Mk lineage and production of mature Mk cells, the support of *Feeder* co-culture alone, during the differentiation stage, is not enough and the presence of cytokines in culture medium is necessary. The lower rates of differentiation ($D_t$) and expansion of non-Mk lineage ($E_t$) and HSC/HPC ($E_h$) for conditions that had cytokines in comparison to the *Feeder* condition also demonstrated that the cross-talk with BM-MSCs naturally favors development of primitive HSC/HPC and non-Mk lineage cells. The values of $E_h$, $D_t$ and $E_t$ were higher when cells were continuously expanded using Z9 condition than when cells pre-expanded 7 days using Z9 and then differentiated using *Cyt* (or *Cyt + Feeder*). This might be due to the presence of SCF and Flt-3 in Z9 cocktail that was previously described to promote monocytic and granulocytic commitments (Case et al., 2006).

The ratio of $E_m$ and $D_p$ between *Cyt + Feeder* (HSC/HPC pre-expanded 7 days using Z9 cocktail and then differentiated using *Cyt + Feeder*) to condition Z9 (in which Z9 cocktail was continuously supplemented during full expansion duration) were 2.4 and 1.7, respectively. This result demonstrated the importance of using the specific cytokines (*e.g.* TPO and IL-3) to promote the late stages of megakaryopoiesis.

To summarize, addition of *Cyt* cocktail to the culture medium during differentiation stage, favored higher values of the rate of expansion and differentiation toward Mk lineage, however co-culture with BM-MSC feeder layer favored the expansion of primitive HSC/HPC and non-Mk lineage. This result supports our previous empirical findings, that is, the supremacy of *Cyt* addition over *Feeder* signaling to have an efficient Mk differentiation process (Hatami et al., 2015).

### 4.3. Flux analysis and the impact of the expansion and differentiation parameters

To gain insights about the evolution of subpopulations during expansion and differentiation stages, we performed flux analyses for each subpopulation.

#### 4.3.1. Mk progenitor population (M)

The two contributions to produce Mk progenitor population (M) are the fluxes of (i) differentiation of HSC/HPC into the Mk progenitor population ($D_m \times H(t)$) and (ii) expansion of Mk progenitor population ($E_m \times M(t)$). The two relative contributions of fluxes during expansion (Fig. 6A) and differentiation (Fig. 6B) are calculated as the ratios of $D_m \times H(t)$ and $E_m \times M(t)$ to the sum of all these parameters, $F_m = D_m \times H(t) + E_m \times M(t)$.

This analysis indicated, for the expansion stage (Fig. 6A), that the small production of Mk progenitor using T0 is entirely limited to the differentiation of HSC/HPC. Indeed, the cocktail used in T0 was unable to sustain or increase in the population of Mk progenitors with negative values of $E_m$ associated to the death of Mk progenitor population. However, the number of Mk progenitors increased over the 14 days of expansion using Z9 condition. The flux analysis demonstrated that in the first 7 days of the expansion stage such increase was mainly due to the contribution of differentiation of HSC/HPC to Mk progenitors. Though, for the second half of the expansion stage, with increase of the Mk progenitor population and decrease of HSC/HPC population, both contributions (*i.e.* differentiation of HSC/HPC and expansion of Mk progenitor) became important.

The flux analysis for 10 days of differentiation (Fig. 6B) demonstrated an increase in contribution of fluxes related with the expansion of Mk progenitors soon after the cells cultured in the differentiation conditions. Interestingly, when the *Cyt* cocktail (TPO + IL3) was used (alone or in combination with *Feeder* layer), the contribution of Mk progenitor expansion was dominant earlier in the culture.

#### 4.3.2. Mature Mk cells (P)

In order to quantify the fraction of the Mk progenitor population produced that differentiated into mature Mk cells (P), the $Z_p$ parameter was calculated according to Eq. (7) and presented in Fig. 6C.

$$Z_p(t) = \frac{D_p.M(t)}{D_m.H(t) + E_m.M(t)} \tag{7}$$

All differentiation conditions and expansion using Z9 showed the increasing ratio of fluxes related with production of mature

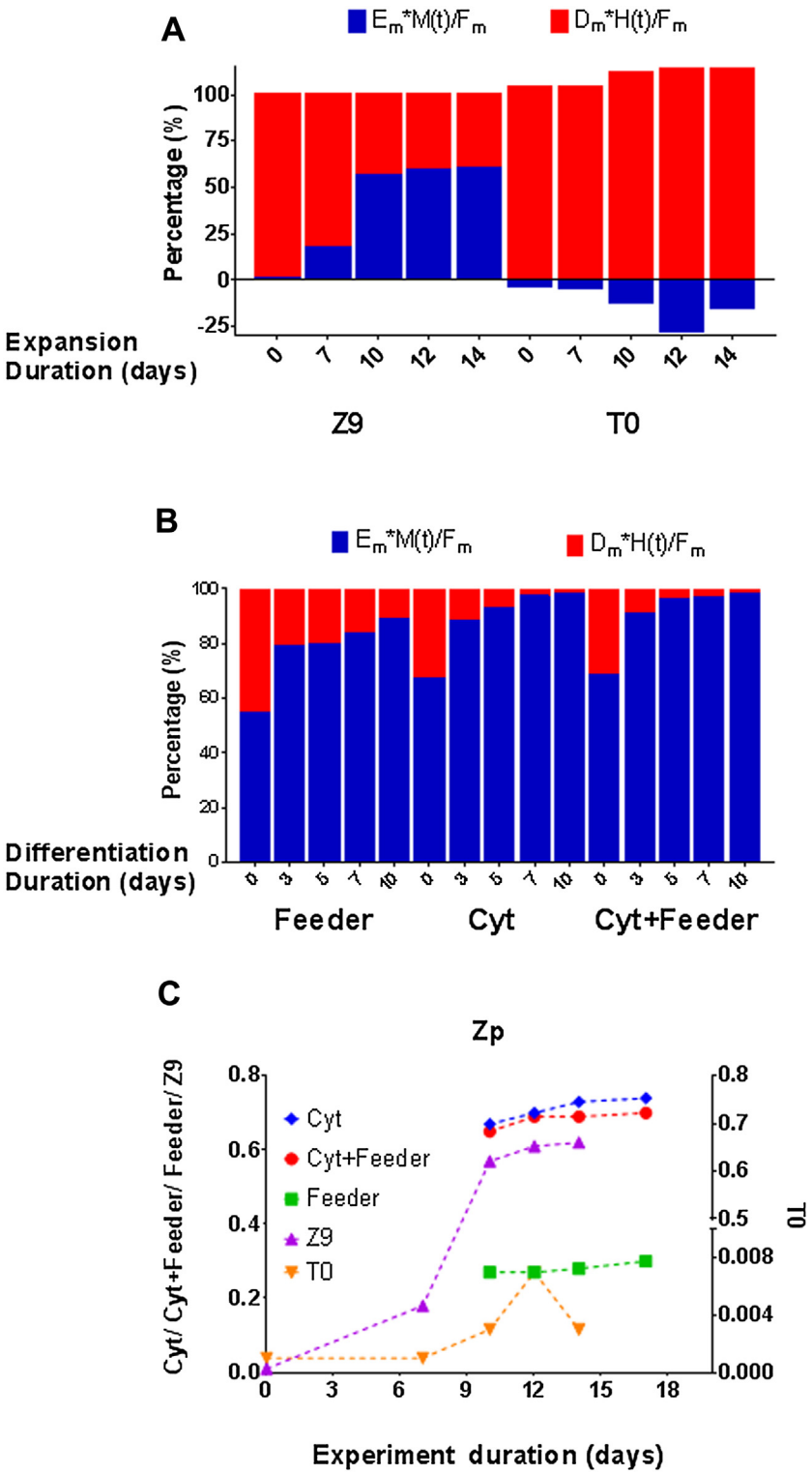


**Fig. 6.** Flux analysis for Mk progenitor population. Percentages of fluxes contributing to increase in M population (measure as $F_m(t) = D_m \times H(t) + E_m \times M(t)$) either due to differentiation of H to M population or expansion of M population during (A) 14 days of expansion and (B) 10 days of differentiation stages are presented as red ($D_m \times H(t)/F_m(t)$) and blue ($E_m \times M(t)/F_m(t)$) bars, respectively. Only cells expanded for 7 days using Z9, in co-culture with BM-MSC, were used for differentiation stage. C) Flux of M population differentiated to mature Mk cells (P) was divided by the fluxes related with the production of M cells as the function of time to estimate Zp (*i.e.* Zp represents the balance between production of the M population and differentiation into the P population in each time instant). (For interpretation of the references to colour in this figure legend, the reader is referred to the web version of this article.)

Mk cells ($D_p \times M(t)$) during experiment duration, with fractions above 0.5 found for the three cocktails that include TPO (*Cyt*, *Cyt + Feeder* and Z9) on the later culture stages. Moreover, all the ratios were below 1, implying that the production of mature Mk cells (P) was not limited for the lack of Mk progenitor (M) cells supply.

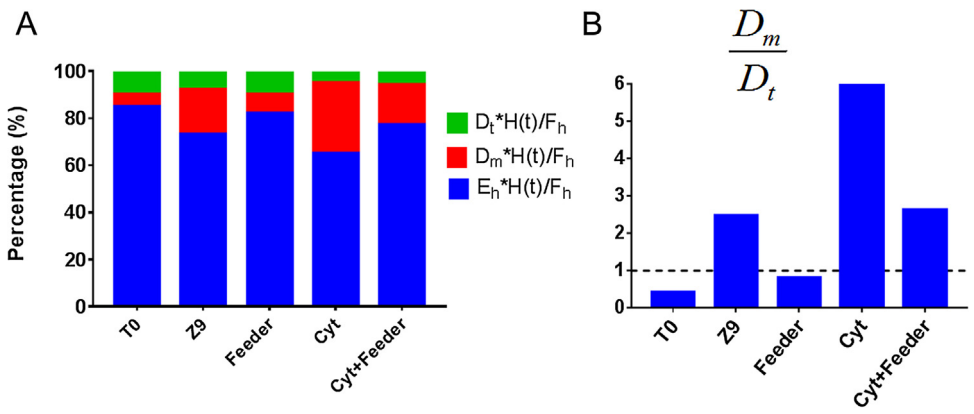


**Fig. 7.** Flux analysis for HSC/HPC population. A) Ratio of fluxes of differentiation of HSC/HPC to T (green bar) and M populations (red bar) and expansion of HSC/HPC (blue bar) population during 14 days of expansion (labeled as Z9 and T0) and 10 days of differentiation stages (labeled as *Cyt*, *Feeder* and *Cyt + Feeder*) are presented. B) Ratio between the rate of differentiation of HSC/HPC to Mk progenitor population ($D_m$) and non-Mk lineage population ($D_t$) is illustrated.

#### 4.3.3. HSC/HPC population (H)

The flux analysis performed for HSC/HPC population (Fig. 7A) considered the fate of such population, to expand (yielding more HSC/HPC) or differentiate to Mk progenitors (M population) or non-Mk cell types (T population). Therefore, the ratio of fluxes of each of these possible fates to the total flux output of HSC/HPCs, herein calculated as $F_h = E_h \times H(t) + D_m \times H(t) + D_t \times H(t)$, were estimated to analyze the contribution of each cell fates during experiment duration. This time-independent result revealed that the ratio of flux related with the expansion of HSC/HPC population was dominant among all expansion and differentiation conditions, which indicates that the HSC/HPCs in this culture are yet very prone self-renewing. This observation implies that the population of $CD34^+CD41^-$ cells (H population) did not exhausted, which could be positive for the long term culture as a source of cells for further differentiation.

To understand the balance between differentiation fate of HSC/HPC to Mk lineage and non-Mk lineage, the ratio between $D_m$ and $D_t$ were illustrated in Fig. 7B. This result displayed that when TPO is always presented in the culture condition (*Cyt*, *Cyt + Feeder* or Z9) the HSC/HPC cells are more differentiated toward Mk lineage (*e.g.* $D_m/D_t > 1$) compare to the TPO-free conditions (*Feeder* and T0). The result also demonstrated that when co-culture with BM-MSC included in the experimental configuration; there was a tendency to shift the differentiation of HSC/HPC toward Non-Mk lineage cells (*e.g.* $D_m/D_t < 1$).

#### 4.3.4. Non-Mk population (T)

Flux analysis for non-Mk population revealed the flux of expansion of this population increased during expansion (Fig. S1A) and differentiation (Fig. S1B) stages and had dominant role over flux of differentiation of HSC/HPC to non-Mk population.

### 4.4. Sensitivity analysis

Sensitivity analysis was performed on each individual cell fate rate coefficient to assess how small changes in cell fate rate coefficient could affect the production yield of megakaryocytic progenitors (M) and mature Mk cells (P). We were able to discriminate between high and low-impact cell fate coefficient rates on the outcome of the megakaryopoiesis process. In Eq. (8), $S_{ij}(t_k)$ is the sensitivity of the desired output of $i$ at time $k$ on the cell fate coefficient rate $j$, $dC_i(t_k)$ is the resulting change in an output $i$ at given time $k$ for the change in a cell fate rate coefficient $j$. $h_j$ is the current value of $j$, $dh_j$ is the change in a cell fate rate coefficient $j$, and $C_i(t_k)$ is the present value of an output $i$ at time $k$ as previously described (Selekman et al., 2013).

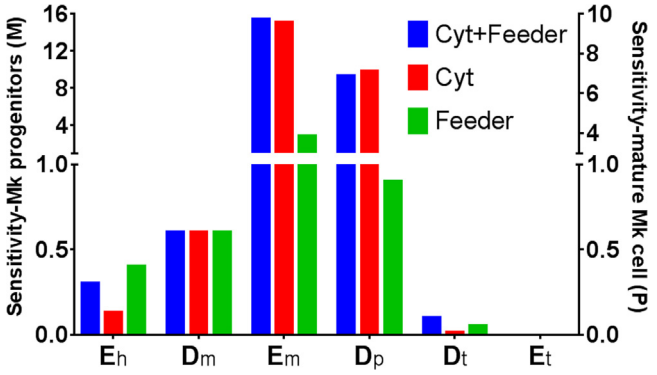


**Fig. 8.** Sensitivity analysis for the differentiation stage calculated according to Eq. (8). Maximum values of the sensitivities were calculated to estimate the 10% change in each individual parameters to the resulting number of Mk progenitors (M, left y axis) and mature Mk cells (P, right y axis) under three differentiation conditions: *Cyt*, *Cyt + Feeder* and *Feeder*.

$$S_{ij}(t_k) = \frac{dC_i(t_k)}{dh_j} \times \frac{h_j}{C_i(t_k)} \tag{8}$$

In the present work, the desired outputs ($C_i(t_k)$) were the total number of megakaryocytic progenitors (M) and mature Mk cells (P) at the end of the differentiation stage. Our aim was to evaluate the impact of a 10% change in the individual parameters (cell fate coefficient rates) on the sensitivity of the output parameters. Initially, all cell fate coefficient rates were fixed and only made 10% change in one of the cell fate coefficient rates, then that parameter was returned to the original value and this process was repeated until all parameters were assessed. Indeed, a random number with ±10% of the initial value of each cell fate coefficient rates was selected and the resulting outputs were calculated according to Eq. (8). This process was repeated (*i.e.* 5000 times) for each cell fate coefficient rates and maximum values of the sensitivity were presented in Fig. 8. These values were calculated for a 10% change in cell fate coefficient rates, for the last day of the differentiation stage, on the number of megakaryocytic progenitors (M) and mature Mk cells (P). The results demonstrated that the final yield of $CD34^+CD41^+$(M cells) and $CD34^-CD41^+$ (P cells) are the most sensitive to small changes in the proliferation rate of Mk progenitors ($E_m$) and differentiation of these cells to mature Mk cells ($D_p$) in all different differentiation protocol (Fig. 8). Interestingly, when *Cyt* was added to the differentiation protocol, alone or in combination with the BM-MSC feeder

layer, the desired outputs (number of M and P cells) were much more sensitive to the changes in the value of $E_m$ and $D_p$ than when only *Feeder* co-culture was used. For example, the numbers of Mk progenitors were 5 times more sensitive to 10% changes in the $D_p$ values when *Cyt* was included in the protocol. Our analysis demonstrated that 1% and 5% changes in the cell fate rate coefficients had the same effect on the sensitivity of the desired outputs during the differentiation stage.

## 5. Discussion

In the present work we developed a computational framework to explore the effect of different biological parameters such as stromal/accessory cells and biochemical cues that mimic the BM niche on the cell fate during the megakaryopoiesis process *ex vivo*. Our model elucidated the effect of the presence of Thrombopoietin (TPO) in the expansion stage on the kinetics of cell expansion and differentiation. Then, the effect of a cross-talk between human MSC and HSC/HPC, in the presence of differentiation cytokines alone or in a synergic fashion, was revealed. Through this model we computed the cell number of each subpopulation as a function of time using four ODEs. In our previous work (Hatami et al., 2015), we described distinct effects of biochemical cues and stromal/accessory cells on the megakaryo/thrombopoiesis process *ex vivo* using UCB cells. However, we were not able to discriminate and quantify the effect of experimental parameters on the efficiency of megakaryopoiesis. In the current work, the computational model gave us a robust tool to quantify and analyze the role of each cell fate coefficient rates on the fate of each population. In other words, we decoupled the kinetic of expansion and differentiation rates using a subpopulation dynamic model. This allowed us to find the most sensitive parameters to establish an efficient megakaryopoiesis process. Using sensitivity analysis, we predicted the most important parameters affecting the total number of Mk progenitors and mature Mk cells in the differentiation stage.

One of the findings of the present work was a quantitative description that step-wise culture of cells is important to have an efficient megakaryopoiesis process. When cells were continuously expanded using Z9 condition, $D_m$ was much higher and, at the same time, $E_m$ and $D_p$ were much lower, in comparison to cells pre-expanded using Z9 for 7 day and then differentiated using *Cyt* or *Cyt + Feeder* condition. Therefore, it was important firstly to culture cells using Z9 cocktail to produce enough amount of Mk progenitors and then transfer these cells to the differentiation conditions (*Cyt* or *Cyt + Feeder*) to promote later stages of megakaryopoiesis (expansion of Mk progenitor and their differentiation to mature Mk cells).

Upon expansion using the Z9 cocktail, regardless the conditions used during the differentiation stage (*Cyt*, *Feeder* or *Cyt + Feeder*), the highest values of $E_m$ when compared to the values of other coefficient rates, demonstrate the important role of Mk progenitors to have an efficient megakaryopoiesis process. The higher value of $D_m$ for the cells continuously expanded using Z9 condition, when compared to the differentiation using *Cyt*, demonstrated that addition of other cytokines, besides TPO, is necessary for early stage of megakaryopoiesis. This observation was described before, when Proulx and collagenous reported that addition of a limited amount of Flt-3 ($\leq$10 ng/mL) to UCB $CD34^+$-enriched cells cultured in a serum-free medium supplemented with TPO and SCF resulted in a 15-fold increase in the number of Mk cells (Proulx et al., 2003).

It is essential to discuss the assumptions made in this study. We assumed a deterministic model of the megakaryopoiesis process, which predicts a similar outcome with different variations associated with random experimental errors. Our aim was not to find the underlying mechanism of differentiation and self-renewal in terms of the stochastic or deterministic nature. However, our model offers a descriptive tool to understand the effect of exogenous signals on the kinetic of megakaryopoiesis and therefore to interpreting the cause-and-effect relationships during *ex vivo* culture of HSC/HPCs. Using population dynamics approach, it was possible to estimate cell fate parameters of the specific cell subpopulations presented in the culture without requiring an understanding of underlying intracellular mechanisms (Prudhomme et al., 2004). Another assumption made here was to consider that all kinetic rate coefficients were independent of time. In fact, paracrine signaling and cell-cell contact could possibly alter these kinetic rates coefficients. However, it should be noted that a prior knowledge of the individual or synergic effects of such parameters as a function of dynamical changes in subpopulation dynamics are not available and so it is unrealistic to build a comprehensive model without having that important information. The computational framework outlined here is useful as a basis to add more complexity or refinement for future inclusive models. We have characterized non-Mk lineage cells (T) with a single proliferation ($E_t$) coefficient rate and HSC/HPS population with a single proliferation ($E_h$) and two differentiation ($D_m$ and $D_t$) coefficient rates. It should be noted that these populations were heterogeneous in their nature. Non-Mk population was defined as all the cells with $CD34^-CD41^-CD42b^-$ phenotype. HSC/HPCs were also population of stem cells and progenitors ($CD34^+$ cells). Therefore, they were comprised by very heterogenic population of cells, potentially contained subpopulations with different proliferation and differentiation rates. As the cell culture progress in time, different kinetic of subpopulations becomes more stringent which resulted in a curve that is not any longer properly described by one or two kinetic parameters. Perhaps that is the main reason our model underpredicted the number of cells in these populations during the differentiation stage (Fig. 4A & C). The outcome for better-defined and more homogeneous populations, Mk progenitor (M) and mature Mk populations (P), yet resulted in a better experimental and model data fitting (Fig. 4B & D). Our focus in this work was to find the important factors affecting the megakaryopoiesis process as a complement to our experimental work and so in the light of this specific aim, a more detailed subpopulation characterization is necessary to understand the dynamical nature of non-Mk lineage population for future studies. Our model did not incorporate the terms related with polyploidy of Mks because, according to our previous study (Hatami et al., 2014) and report by others (Mattia et al., 2002), Mks generated from UCB had low ploidy level (mainly with DNA content $\leq$ 4N). This phenomenon was previously studied, and though with low level of ploidy, Mks generated from UCB were fully functional and able to produce platelets (Mattia et al., 2002).

Our computational model was able to deconvolute data from cell number and flow cytometry to different subpopulation specific rates, describing self-renewal and differentiation. As a result of the computational modeling performed here, we found that the expansion coefficient rate of Mk progenitors ($E_m$) and Differentiation coefficient rate of Mk progenitors to mature Mk cells ($D_p$) are the two most important factors that should be considered to design an efficient megakaryopoiesis process. This kind of approach has also been previously performed to find an efficient protocol for the differentiation of human pluripotent stem cells (Selekman et al., 2013). The result of the current study could be useful in designing a multi-stage protocol (such as commitment ► proliferation ► maturation), in which the growth and maturation of Mks should be optimized to achieve the highest yield of the megakaryopoiesis process. In order to achieve the best yield for Mk and platelet production, one possible approach to manipulate $D_m$, $E_m$ and $D_p$ is to include the specific cytokines and signaling molecules in the culture cocktail that were demonstrated to affect the proliferation of Mk progenitors (*i.e.* IL-3, IL-6, IL-11, SCF), their differentiation

and fully maturation of Mk cells (*i.e.* TPO, SDF-1)(Avecilla et al., 2004; Burstein et al., 1992; Lazzari et al., 2000; Proulx et al., 2003; Williams et al., 1998).

In order to build a comprehensive *in silico* model of BM niche that could explain the megakaryopoiesis process, prospect computational models should consider relevant physio-chemical and biological factors presented in the niche such as oxygen level, geometry of the system (3D *vs*. 2D), polyploidy of Mks and the interaction between different subset of niche (*e.g.* direct and indirect cell-cell contact) (Fuentes-Gari et al., 2015; Roeder, 2006; Viswanathan and Zandstra, 2003).

## 6. Conclusion

Developing descriptive-predictive computational models is important for a rational design of experiments for high-level screening of culture parameters (Kirouac and Zandstra, 2008). This could be implemented into the empirical models that describe the bioprocess outputs as the multiple culture parameters. Ultimately, this approach may provide a means to find the most sensitive culture parameters and will offer a robust solution to establish optimized process settings (Audet et al., 2002). One of the crucial challenges in an *in vitro* production of platelets is to produce a stable progenitor intermediate or a self-renewing megakaryocyte progenitor population that can be quickly driven to maturation for platelet production (Sim et al., 2016). Our computational approach offers a quantitative way to measure the rate of differentiation of HSC/HPC to Mk progenitor ($D_m$) and subsequent differentiation to mature Mk cells ($D_p$). Therefore, it is possible to implement our computational model to design specefic experiments and to screen possible candidates to enhance production of such important intermediate population.

## Acknowledgements

This work was financially supported by Fundação para a Ciência e a Tecnologia (FCT), Portugal through a PhD scholarship (SFRH/BD/61450/2009) awarded to JH, the research project titled "Mathematical and Computational Modeling of Human Physiology: PHYSIOMATH" – EXCL/MAT-NAN/0114/2012 and Center for Computational and Stochastic Mathematics (CEMAT), Universidade de Lisboa (Lisbon, Portugal) and MIT Portugal Program. Funding to iBB-Institute for Bioengineering and Biosciences by FCT (UID/BIO/04565/2013 and from Programa Operacional Regional de Lisboa 2020 (LISBOA-01-0145-FEDER-007317) is acknowledged.

## Appendix A. Supplementary data

Supplementary data associated with this article can be found, in the online version, at http://dx.doi.org/10.1016/j.compchemeng.2016.07.027.

## References

Akashi, K., He, X., Chen, J., Iwasaki, H., Niu, C., Steenhard, B., Zhang, J., Haug, J., Li, L., 2003. Transcriptional accessibility for genes of multiple tissues and hematopoietic lineages is hierarchically controlled during early hematopoiesis. Blood 101, 383–389.

Andrade, P.Z., dos Santos, F., Almeida-Porada, G., da Silva, C.L., Cabral J.M, S., 2010. Systematic delineation of optimal cytokine concentrations to expand hematopoietic stem/progenitor cells in co-culture with mesenchymal stem cells. Mol. Biosyst. 6, 1207–1215.

Audet, J., Miller, C.L., Eaves, C.J., Piret, J.M., 2002. Common and distinct features of cytokine effects on hematopoietic stem and progenitor cells revealed by dose-response surface analysis. Biotechnol. Bioeng. 80, 393–404.

Avecilla, S.T., Hattori, K., Heissig, B., Tejada, R., Liao, F., Shido, K., Jin, D.K., Dias, S., Zhang, F., Hartman, T.E., Hackett, N.R., Crystal, R.G., Witte, L., Hicklin, D.J., Bohlen, P., Eaton, D., Lyden, D., de Sauvage, F., Rafii, S., 2004. Chemokine-mediated interaction of hematopoietic progenitors with the bone marrow vascular niche is required for thrombopoiesis. Nat. Med. 10, 64–71.

Bartolini, E., Manoli, H., Costamagna, E., Jeyaseelan, H.A., Hamad, M., Irhimeh, M.R., Khademhosseini, A., Abbas, A., 2015. Population balance modelling of stem cell culture in 3D suspension bioreactors. Chem. Eng. Res. Des. 101, 125–134.

Boulais, P.E., Frenette, P.S., 2015. Making sense of hematopoietic stem cell niches. Blood 125, 2621–2629.

Bryder, D., Rossi, D.J., Weissman, I.L., 2006. Hematopoietic stem cells: the paradigmatic tissue-specific stem cell. Am. J. Pathol. 169, 338–346.

Burstein, S.A., Mei, R.L., Henthorn, J., Friese, P., Turner, K., 1992. Leukemia inhibitory factor and interleukin-11 promote maturation of murine and human megakaryocytes in vitro. J. Cell. Physiol. 153, 305–312.

Caldwell, J., Wang, W., Zandstra, P.W., 2015. Proportional-Integral-Derivative (PID) control of secreted factors for blood stem cell culture. PLoS One 10, e0137392.

Case, J., Hicks, C., Trickett, A., Kwan, Y.L., Manoharan, A., 2006. The expansion of megakaryocyte progenitors from CD34$^+$-enriched mobilized peripheral blood stem cells is inhibited by Flt3-L. J. Interferon. Cytokine. Res. 26, 76–82.

Ceredig, R., Rolink, A.G., Brown, G., 2009. Models of haematopoiesis: seeing the wood for the trees. Nat. Rev. Immunol. 9, 293–300.

Cross, M.A., Enver, T., 1997. The lineage commitment of haemopoietic progenitor cells. Curr. Opin. Genet. Dev. 7, 609–613.

Deutsch, V.R., Tomer, A., 2013. Advances in megakaryocytopoiesis and thrombopoiesis: from bench to bedside. Br. J. Haematol. 161, 778–793.

Fuentes-Gari, M., Velliou, E., Misener, R., Pefani, E., Rende, M., Panoskaltsis, N., Mantalaris, A., Pistikopoulos, E.N., 2015. A systematic framework for the design, simulation and optimization of personalized healthcare: making and healing blood. Comput. Chem. Eng. 81, 80–93.

Glauche, I., Cross, M., Loeffler, M., Roeder, I., 2007. Lineage specification of hematopoietic stem cells: mathematical modeling and biological implications. Stem Cells 25, 1791–1799.

Gullo, F., van der Garde, M., Russo, G., Pennisi, M., Motta, S., Pappalardo, F., Watt, S., 2015. Computational modeling of the expansion of human cord blood CD133$^+$ hematopoietic stem/progenitor cells with different cytokine combinations. Bioinformatics 31, 2514–2522.

Hatami, J., Andrade, P.Z., Bacalhau, D., Cirurgião, F., Ferreira, F.C., Cabral, J.M.S., da Silva, C.L., 2014. Proliferation extent of CD34$^+$ cells as a key parameter to maximize megakaryocytic differentiation of umbilical cord blood-derived hematopoietic stem/progenitor cells in a two-stage culture protocol. Biotechnol. Rep. 4, 50–55.

Hatami, J., Andrade, P.Z., Alves de Matos, A.P., Djokovic, D., Lilaia, C., Ferreira, F.C., Cabral, J.M.S., da Silva, C.L., 2015. Developing a co-culture system for effective megakaryo/thrombopoiesis from umbilical cord blood hematopoietic stem/progenitor cells. Cytotherapy 17, 428–442.

Kawamoto, H., Ikawa, T., Masuda, K., Wada, H., Katsura, Y., 2010. A map for lineage restriction of progenitors during hematopoiesis: the essence of the myeloid-based model. Immunol. Rev. 238, 23–36.

Kirouac, D.C., Zandstra, P.W., 2008. The systematic production of cells for cell therapies. Cell Stem Cell 3, 369–381.

Kirouac, D.C., Madlambayan, G.J., Yu, M., Sykes, E.A., Ito, C., Zandstra, P.W., 2009. Cell-cell interaction networks regulate blood stem and progenitor cell fate. Mol. Syst. Biol. 5, 293.

Kondo, M., 2010. Lymphoid and myeloid lineage commitment in multipotent hematopoietic progenitors. Immunol. Rev. 238, 37–46.

Kresnowati, M.T., Forde, G.M., Chen, X.D., 2011. Model-based analysis and optimization of bioreactor for hematopoietic stem cell cultivation. Bioprocess. Biosyst. Eng. 34, 81–93.

Lai, A.Y., Kondo, M., 2006. Asymmetrical lymphoid and myeloid lineage commitment in multipotent hematopoietic progenitors. J. Exp. Med. 203, 1867–1873.

Laiosa, C.V., Stadtfeld, M., Graf, T., 2006. Determinants of lymphoid-myeloid lineage diversification. Annu. Rev. Immunol. 24, 705–738.

Lazzari, L., Henschler, R., Lecchi, L., Rebulla, P., Mertelsmann, R., Sirchia, G., 2000. Interleukin-6 and interleukin-11 act synergistically with thrombopoietin and stem cell factor to modulate ex vivo expansion of human CD41$^+$ and CD61$^+$ megakaryocytic cells. Haematologica 85, 25–30.

Leslie, M., 2010. Cell biology: beyond clotting: the powers of platelets. Science 328, 562–564.

Loeffler, M., Wichmann, H.E., 1980. A comprehensive mathematical-model of stem-cell proliferation which reproduces most of the published experimental results. Cell Tissue Kinet. 13, 543–561.

Manesso, E., Teles, J., Bryder, D., Peterson, C., 2013. Dynamical modelling of haematopoiesis: an integrated view over the system in homeostasis and under perturbation. J. R. Soc. Interface 10, 20120817.

Mattia, G., Vulcano, F., Milazzo, L., Barca, A., Macioce, G., Giampaolo, A., Hassan, H.J., 2002. Different ploidy levels of megakaryocytes generated from peripheral or cord blood CD34$^+$ cells are correlated with different levels of platelet release. Blood 99, 888–897.

Morrison, S.J., Scadden, D.T., 2014. The bone marrow niche for haematopoietic stem cells. Nature 505, 327–334.

Naik, S.H., Perie, L., Swart, E., Gerlach, C., van Rooij, N., de Boer, R.J., Schumacher, T.N., 2013. Diverse and heritable lineage imprinting of early haematopoietic progenitors. Nature 496, 229–232.

Notta, F., Zandi, S., Takayama, N., Dobson, S., Gan, O.I., Wilson, G., Kaufmann, K.B., McLeod, J., Laurenti, E., Dunant, C.F., McPherson, J.D., Stein, L.D., Dror, Y., Dick, J.E., 2016. Distinct routes of lineage development reshape the human blood hierarchy across ontogeny. Science 351, aab2116.

Peng, C.-A., Koller, M.R., Palsson, B.Ø., 1996. Unilineage model of hematopoiesis predicts self-renewal of stem and progenitor cells based on ex vivo growth data. Biotechnol. Bioeng. 52, 24–33.
Pineault, N., Boisjoli, G.J., 2015. Megakaryopoiesis and ex vivo differentiation of stem cells into megakaryocytes and platelets. ISBT Sci. Ser. 10, 154–162.
Proulx, C., Boyer, L., Hurnanen, D.R., Lemieux, R., 2003. Preferential ex vivo expansion of megakaryocytes from human cord blood $CD34^+$-enriched cells in the presence of thrombopoietin and limiting amounts of stem cell factor and Flt-3 ligand. J. Hematother. Stem Cell Res. 12, 179–188.
Prudhomme, W.A., Duggar, K.H., Lauffenburger, D.A., 2004. Cell population dynamics model for deconvolution of murine embryonic stem cell self-renewal and differentiation responses to cytokines and extracellular matrix. Biotechnol. Bioeng. 88, 264–272.
Psaila, B., Barkas, N., Iskander, D., Roy, A., Anderson, S., Ashley, N., Caputo, V.S., Lichtenberg, J., Loaiza, S., Bodine, D.M., Karadimitris, A., Mead, A.J., Roberts, I., 2016. Single-cell profiling of human megakaryocyte-erythroid progenitors identifies distinct megakaryocyte and erythroid differentiation pathways. Genome Biol. 17, 83.
Reems, J.-A., Pineault, N., Sun, S., 2010. In vitro megakaryocyte production and platelet biogenesis: state of the art. Transfus. Med. Rev. 24, 33–43.
Roeder, I., 2006. Quantitative stem cell biology: computational studies in the hematopoietic system. Curr. Opin. Hematol. 13, 222–228.
Rondina, M.T., Weyrich, A.S., Zimmerman, G.A., 2013. Platelets as cellular effectors of inflammation in vascular diseases. Circ. Res. 112, 1506–1519.
Seita, J., Weissman, I.L., 2010. Hematopoietic stem cell: self-renewal versus differentiation. Wiley Interdiscip. Rev. Syst. Biol. Med. 2, 640–653.
Selekman, J.A., Das, A., Grundl, N.J., Palecek, S.P., 2013. Improving efficiency of human pluripotent stem cell differentiation platforms using an integrated experimental and computational approach. Biotechnol. Bioeng. 110, 3024–3037.
da Silva, C.L., Goncalves, R., Lemos, F., Lemos, M.A., Zanjani, E.D., Almeida-Porada, G., Cabral, J.M., 2003. Modelling of ex vivo expansion/maintenance of hematopoietic stem cells. Bioprocess. Biosyst. Eng. 25, 365–369.
Sim, X., Poncz, M., Gadue, P., French, D.L., 2016. Understanding platelet generation from megakaryocytes: implications for in vitro-derived platelets. Blood 127, 1227–1233.
Stiehl, T., Baran, N., Ho, A.D., Marciniak-Czochra, A., 2015. Cell division patterns in acute myeloid leukemia stem-like cells determine clinical course: a model to predict patient survival. Cancer. Res. 75, 940–949.
Stroncek, D.F., Rebulla, P., 2007. Platelet transfusions. Lancet 370, 427–438.
Thon, J.N., Medvetz, D.A., Karlsson, S.M., Italiano Jr., J.E., 2015. Road blocks in making platelets for transfusion. J. Thromb. Haemost. 13 (Suppl. 1), S55–62.
Viswanathan, S., Zandstra, P.W., 2003. Towards predictive models of stem cell fate. Cytotechnology 41, 75–92.
Viswanathan, S., Davey, R.E., Cheng, D., Raghu, R.C., Lauffenburger, D.A., Zandstra, P.W., 2005. Clonal evolution of stem and differentiated cells can be predicted by integrating cell-intrinsic and −extrinsic parameters. Biotechnol. Appl. Biochem. 42, 119–131.
Whichard, Z.L., Sarkar, C.A., Kimmel, M., Corey, S.J., 2010. Hematopoiesis and its disorders: a systems biology approach. Blood 115, 2339–2347.
Williams, J.L., Pipia, G.G., Datta, N.S., Long, M.W., 1998. Thrombopoietin requires additional megakaryocyte-active cytokines for optimal ex vivo expansion of megakaryocyte precursor cells. Blood 91, 4118–4126.